ISSN: 2181-3337 | SCIENTISTS.UZ VOLUME 5 ISSUE 8 AUGUST 2026

DEFORMATION-DECOUPLED CONNECTIONS BETWEEN A PULTRUDED GFRP FRAME AND THREE-LAYER 3D-PRINTED WALLS

Analytical design methodology and a reproducible benchmark study

Akbarov Dilshod[1], **Akramov Khusnitdin**
[1]Tashgiprogor LLC, Tashkent, Uzbekistan; Chief Project Engineer;
M.Sc. in Production of Building Materials, Products and Structures;
[2]Department of Technology of Building Materials and Structures,
Tashkent University of Architecture and Civil Engineering, Tashkent, Uzbekistan;
Doctor of Technical Sciences, Professor; e-mail: x.akromov@taqu.uz;
* Corresponding author: dilshodakbarov0@gmail.com

DOI: 10.67620/sai.58a0002

ABSTRACT

Pultruded glass-fiber-reinforced polymer (GFRP) frames and additively manufactured wall panels respond differently to temperature, shrinkage, and interstory drift. A rigid link between them can make a nominally non-load-bearing wall participate in the lateral system and can initiate brittle damage around fasteners or printed interlayers. This paper develops an analytical design procedure for a deformation-decoupled interface in which wall weight, out-of-plane restraint, and in-plane movement are assigned to separate components. The study is deliberately numerical; no laboratory results are reported. A reproducible two-story benchmark building in Tashkent is used to demonstrate the procedure. Loads are derived from stated geometry, densities, and design combinations rather than introduced as free numerical inputs. The original four-bolt U1 detail is reassessed against bearing, net-section tension, shear-out, cleavage, block-shear, bolt-shear, and local interlaminar-screening limit states. With EN 13706 E23 minimum properties and ASCE/SEI 74-23 resistance factors, a conventional hollow-wall through-bolt arrangement is inadequate because the tube-wall bearing reduction governs. A revised seated cleat with internal backing plates, spacer sleeves, and two M16 bolts on each of two symmetric side plates satisfies the short-duration 35.0 kN reaction and the sustained-load check; the highest sustained-load utilization is 0.94. For a 3.6 × 3.0 m wall module, the factored weight is 22.95 kN and the reaction at each of four lower supports is 7.46 kN. A stated wind-load envelope gives 1.20 kPa and 3.24 kN per side anchor. The required one-sided travel is 37.52 mm when no unverified elastic allowance is deducted, leading to a 95 mm slot. A 10% wall-participation limit is derived from a 5% cap on period reduction rather than adopted as an unexplained constant. The paper separates analytical conclusions from the tests still required before construction use.

ACCEPTED

03.09.26

Keywords: *pultruded GFRP; concrete 3D printing; bolted connection; sliding anchor; interstory drift; deformation compatibility; non-load-bearing wall; limit-state design.*

CC BY

Introduction

Pultruded GFRP profiles and additively manufactured cementitious walls are attractive for low-rise construction for different reasons. The frame offers a high strength-to-weight ratio and resistance to corrosion, whereas layer-wise printing reduces formwork and allows service channels or local thickening to be integrated into the wall geometry. These advantages do not automatically make the two subsystems compatible. The frame is expected to resist gravity and lateral actions; the exterior wall is expected to carry its own weight, remain stable out of plane, and keep the envelope weather-tight. If a rigid bracket inadvertently couples their in-plane movements, the wall can behave as an unintended diagonal strut and the structural model changes after construction (Bos et al., 2022; Erdem et al., 2021; Federal Emergency Management Agency, 2012; International Organization for Standardization & ASTM International, 2023; Wolfs et al., 2023).

The local mechanics are also dissimilar. A pultruded profile is orthotropic and has little capacity for plastic redistribution around a hole. Bearing, net-section rupture, shear-out, cleavage, block shear, washer pull-through, and local wall collapse may compete in the same joint (American Society of Civil Engineers, 2023; Eskenati et al., 2022; European Committee for Standardization, 2002, 2022; Girão Coelho & Mottram, 2015; Martins et al., 2021a, 2021b, 2023; Matharu & Mottram, 2017; Pirchio et al., 2024; Qureshi, 2022; Qureshi et al., 2020). A printed shell has directional interfaces between beads and layers; a concentrated anchor force may initiate local crushing, splitting, or interlayer separation. A polystyrene-concrete core can distribute load only if the embedded component is deliberately connected to it. Treating the assembly as a conventional steel bracket fixed to an ordinary concrete wall therefore conceals the governing links in the load path.

The scope of the paper is deliberately limited to a completed analytical study and one fully specified benchmark case. No laboratory test, raw measurement, repeated specimen, or statistical result is claimed. The quantities used in the calculations are fixed in the benchmark definition, and each numerical action is derived from stated geometry, material class, and design assumptions. The experimental program is reported only as the verification still required before a prototype can be used in construction.

The work has five objectives: (1) separate the transfer of wall weight, out-of-plane force, and in-plane movement; (2) re-check connection U1 against the relevant brittle failure modes rather than bearing alone; (3) derive the actions used to size U2-U4; (4) express accidental wall engagement through a gap law and a transparent stiffness criterion; and (5) define construction controls and the tests that remain necessary before the system can be used in a building. The outcome is a design procedure, not a certificate for a particular product.

2. Connection system and benchmark definition

2.1. Functional separation of the interface

The connection system follows one organizing rule: support separately, restrain separately, and allow movement separately. U1 joins the frame members; U2 carries the wall module at its lower edge; U3 and U4 restrain the wall normal to its plane but contain a geometric free-travel zone in the direction of interstory movement; U5 maintains movement and sealing at panel joints, corners, and openings; U6 provides dedicated attachment points for services and façade accessories. The classification prevents one concealed fastener from being assigned mutually incompatible tasks.

ISSN: 2181-3337 | SCIENTISTS.UZ

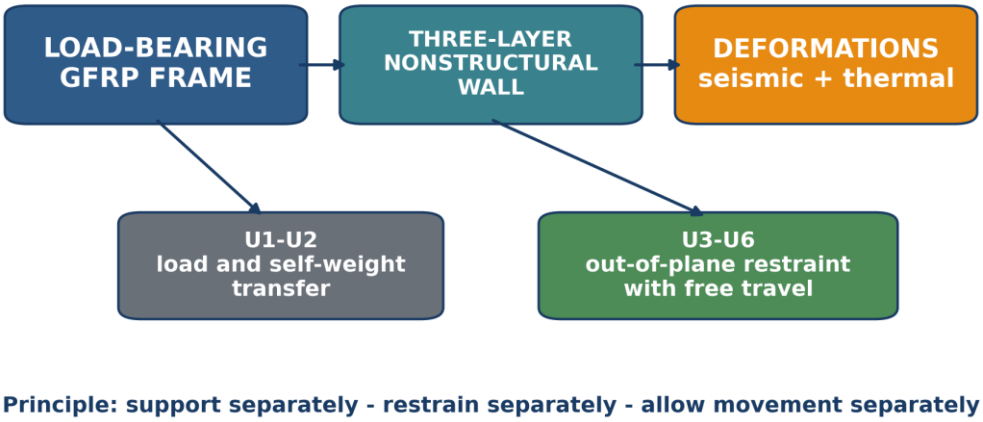


Figure 1. Functional separation of the load paths at the GFRP frame-to-wall interface.

Code	Primary function	Transferred action	Required freedom / control
U1	Beam-to-column frame joint	Beam reaction and erection forces	Predictable strength hierarchy; replaceable steel seat
U2	Lower wall support	Wall self-weight	Independent level adjustment and drainage
U3	Top sliding restraint	Out-of-plane force	Horizontal in-plane travel
U4	Side sliding restraint	Out-of-plane force	Travel parallel to interstory movement
U5	Panel joint, corner, opening	Local façade forces and sealing	Movement joint; two-stage weather seal
U6	Services and secondary attachments	Equipment / façade loads	No intersection with the U3-U5 movement path

Table 1. Functional classification of connections U1-U6.

2.2. Geometry and material data of the worked benchmark

The benchmark is a two-story building with a 10.8 × 7.2 m plan, 3.6 m framing bays, and a 3.0 m story height. It is not presented as an as-built project. Its purpose is to make the analytical sequence reproducible. The wall module is 3.6 m wide and 3.0 m high. Two 30 mm printed shells enclose a 190 mm D350 polystyrene-concrete core. The shell density is set at 1900 kg/m³ and the core density at 350 kg/m³; consequently, the areal mass is $2(0.03)(1900) + 0.19(350) = 180.5$ kg/m².

The GFRP calculations use the minimum characteristic values of EN 13706 class E23 rather than an unreferenced material strength. The chosen values are deliberately conservative: longitudinal tensile strength 240 MPa, transverse tensile strength 50 MPa, longitudinal pin-bearing strength 150 MPa, transverse pin-bearing strength 70 MPa, and in-plane shear strength 25 MPa (European Committee for Standardization, 2002). These class minima describe the benchmark material; they are not a substitute for the certificate and batch tests of a future manufacturer.

ISSN: 2181-3337 | SCIENTISTS.UZ

Parameter	Symbol	Benchmark value	Role in the analysis
Plan dimensions	L × B	10.8 × 7.2 m	Global seismic weight and bay layout
Story height	h	3.0 m	Interstory displacement
Bay / panel width	b	3.6 m	Tributary area and wall module
GFRP column	-	200 × 200 × 12 mm	U1 support member
GFRP beam	-	300 × 150 × 12 mm	Benchmark floor beam
Wall layers	$t_1/tc/t_2$	30/190/30 mm	Mass and local anchorage layout
Printed-shell density	ρs	1900 kg/m³	Declared benchmark input
Core density	ρc	350 kg/m³	D350 benchmark core
Wall areal mass	mA	180.5 kg/m²	Derived from layer thicknesses and densities
GFRP property class	-	EN 13706 E23 minima	Reference strengths for U1
Bolts	-	M16, class 8.8	U1 fasteners; threads excluded from bearing zone

Table 2. Fixed inputs of the reproducible benchmark.

3. Analytical method

3.1. Derivation of the design actions

The U1 beam reaction is obtained from the floor geometry and a stated load combination. The tributary area of one end reaction is one-half of a 3.6 × 3.6 m bay. The characteristic permanent and variable floor loads are 2.5 and 1.5 kPa, respectively. With the LRFD combination 1.2G + 1.6Q, which is consistent with the resistance format used for ASCE/SEI 74-23, the reaction is:

$$VEd = [1.2(2.5) + 1.6(1.5)](3.6 \times 3.6)/2 = 34.99 \approx 35.0\ kN \quad (1)$$

The dead-load-only combination used for the sustained-load check is 1.4G, giving VD = 22.68 kN. Two symmetric U1 seat side plates are assumed to share these reactions equally; each plate and each connected column face is therefore checked for 17.50 kN under the short-duration combination and 11.34 kN under sustained loading.

The wall weight follows directly from the derived areal mass. The design value uses a factor of 1.20, while the lower-support reaction includes a 1.30 non-uniformity factor to cover initial level differences among four adjustable shoes:

$$Gd = 1.20\ mA\ b\ h\ g = 1.20(180.5)(3.6)(3.0)(9.81)/1000 = 22.95\ kN \quad (2)$$

$$RU2,Ed = 1.30\ Gd / 4 = 7.46\ kN\ per\ lower\ support \quad (3)$$

For the façade anchor example, the site basic pressure is fixed at w0 = 0.38 kPa. The product of the design factor, exposure factor, and net pressure coefficient is 1.4 × 1.25 × 1.80. This stated envelope gives q⊥ = 1.197 kPa, rounded to 1.20 kPa. The result is not a universal pressure for Tashkent; it applies to the coefficient set defined here and must be recalculated for another height, exposure, or wall zone (American Society of Civil Engineers, 2022; Republic of Uzbekistan, 2025). Six side anchors are used, and a 1.50 distribution factor accounts for unequal engagement:

ISSN: 2181-3337 | SCIENTISTS.UZ

$$RU4,Ed = 1.50\, q_{\perp}\, b\, h / 6 = 1.50(1.20)(3.6)(3.0)/6 = 3.24\ kN \quad (4)$$

The 28 kN story shear is likewise derived. A 3.0 kPa seismic weight over the 10.8 × 7.2 m floor gives Wstory = 233.28 kN. A benchmark lateral coefficient Cs = 0.12 produces Vstory = 27.99 kN, rounded to 28.0 kN. This value is used only to illustrate the wall-participation criterion; it is not offered as a substitute for a project-specific modal response-spectrum analysis.

Quantity	Derivation	Result
U1 short-duration beam reaction	[1.2(2.5) + 1.6(1.5)] × 12.96 / 2	35.0 kN
U1 sustained dead-load reaction	1.4(2.5) × 12.96 / 2	22.68 kN
Factored wall weight	1.20 × 180.5 × 10.8 × 9.81 / 1000	22.95 kN
One U2 support reaction	1.30 × 22.95 / 4	7.46 kN
Out-of-plane pressure	1.4 × 0.38 × 1.25 × 1.80	1.20 kPa
One U4 anchor action	1.50 × 1.20 × 10.8 / 6	3.24 kN
Benchmark story shear	0.12 × 3.0 × 10.8 × 7.2	28.0 kN

Table 3. Traceable derivation of the numerical actions used in the study.

3.2. U1 limit-state equations and reduction factors

U1 is checked in accordance with the bearing-type connection provisions summarized in ASCE/SEI 74-23 and the accompanying reliability study (American Society of Civil Engineers, 2023; Pirchio et al., 2024). For a connection force parallel to the column pultrusion direction, the benchmark uses Fbr = 150 MPa, Ft = 240 MPa, and Fsh = 25 MPa. The resistance factors are 0.60 for bearing, 0.50 for longitudinal net tension in a multi-row group, 0.45 for two-row shear-out, 0.50 for cleavage, and 0.45 for block shear. A time-effect factor λ = 0.40 is applied to the dead-load-only check. Moisture, temperature, and chemical factors are taken as 1.0 because the benchmark assumes an internal, dry, temperature-controlled connection; a real exterior detail may require lower values.

The revised side-plate geometry on one column face has two M16 bolts in the load direction, 18 mm holes, wall thickness t = 12 mm, end distance e1 = 90 mm, pitch s = 80 mm, side distance e2 = 70 mm, and effective width w = 140 mm. The nominal resistances used in the numerical check are:

$$Rbr = nb\, t\, d\, Fbr \quad (5)$$

$$Rnt = 0.2\, w\, t\, Ft \quad (6)$$

$$Rsh = 1.4(e1 + s - dn/2)tFsh \quad (7)$$

$$Rcl,a = 0.15[(2e2 - dn)Ft + 2e1Fsh]t \quad (8)$$

$$Rcl,b = (10/9 - 4dn/9e1)^2\, Rbr,bolt \quad (9)$$

$$Rbs = 0.5(AnsFsh + AntFt) \quad (10)$$

The design resistance is Rd = φλCRn, where λ = 1.0 for the short-duration combination and 0.40 for the sustained combination. The original hollow-tube detail had washers only on the exterior side of each wall. ASCE/SEI 74-23 requires a 50% bearing reduction for that condition. The revised detail places an internal backing plate against the column wall and uses machined spacer sleeves, so the wall is clamped between two load-distribution surfaces. Omission of the one-sided-wall reduction is therefore an explicit feature of the revised detail, not an unspoken assumption. It still has to be confirmed by a full-scale connection test.

ISSN: 2181-3337 | SCIENTISTS.UZ

3.3. Kinematic model of U3-U4

The sliding restraint is represented by a geometric gap, not by an arbitrarily soft spring. The one-sided travel g contains the interstory displacement, thermal movement, wall shortening, and erection tolerance. No beneficial bracket elasticity is deducted because it has not been measured:

$$g = \theta d\, h + \alpha \Delta T L + \varepsilon sh L + \Delta tol \quad (11)$$

For θd = 1.0%, h = 3000 mm, α = 10 × 10⁻⁶/K, ΔT = 30 K, L = 3600 mm, εsh = 0.0004, and Δtol = 5 mm, the components are 30.00, 1.08, 1.44, and 5.00 mm. Thus g = 37.52 mm. With a 14 mm slot width for an M12 sliding bolt, the calculated symmetric length is 14 + 2(37.52) = 89.04 mm. A 95 mm slot is adopted to provide a manufacturing and rounding reserve.

The global model uses a piecewise law. In-plane force is zero, apart from separately calibrated friction, while $|\Delta| \le g$. After contact with a slot end, the bracket and embedded cassette are mobilized. This distinction matters because a flexible strip that acts from zero displacement can still attract a large part of the story shear.

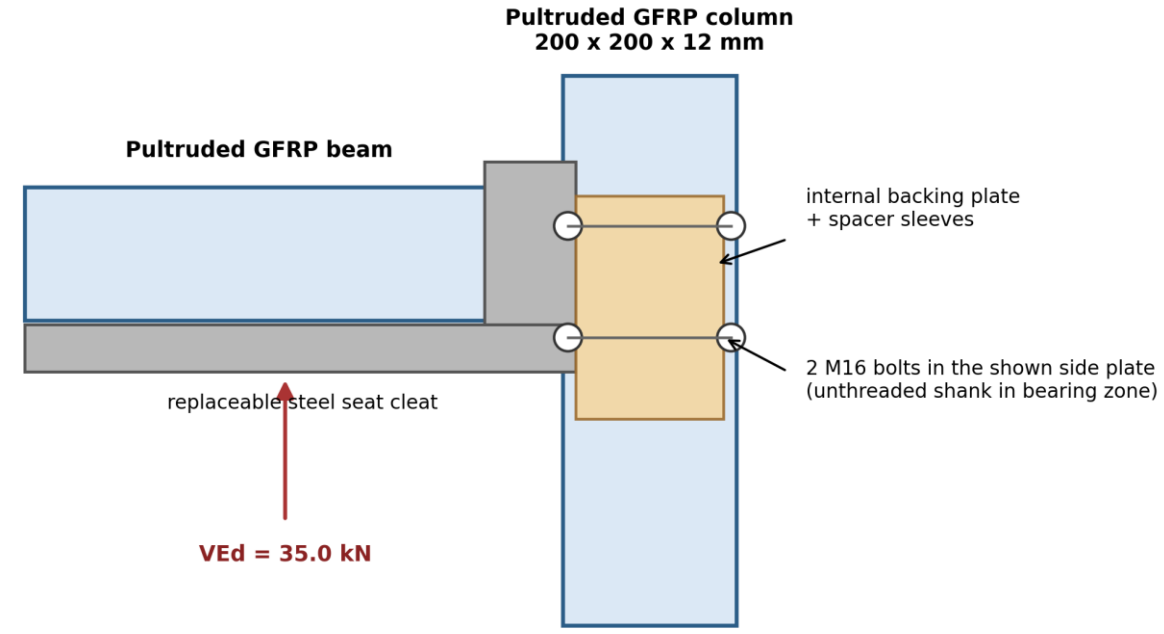
$$F(\Delta) = 0 \text{ for } |\Delta| \le g;\ F(\Delta) = sign(\Delta)\, min[Kc(|\Delta| - g), Rcap] \text{ for } |\Delta| > g \quad (12)$$

4. Results of the worked benchmark

4.1. U1 beam-to-column seat connection

A bearing-only calculation indicates a utilization below unity, but the complete limit-state check changes that conclusion. For four M16 bolts in a hollow column with exterior washers only, the ASCE tube-wall reduction gives a total short-duration bearing resistance of 34.56 kN, slightly less than the 35.0 kN demand. More importantly, the λ = 0.40 sustained resistance is 13.82 kN, compared with 22.68 kN. The unbacked arrangement is therefore rejected.

Figure 2 shows the revised seat. The vertical reaction is carried by the replaceable steel seat, two symmetric side plates share the force, and every bolt has an unthreaded shank through the bearing zone. An internal backing plate and exact-length sleeve are installed before tightening. The connection is thus not dependent on local compression of an unsupported tube wall.



One of two symmetric seat side plates is shown. Each plate carries one-half of the beam reaction.

ISSN: 2181-3337 | SCIENTISTS.UZ

Figure 2. Revised U1 seat detail; one of two symmetric side plates is shown.

Parameter	Value
Demand per column face, short-duration	17.50 kN
Demand per column face, sustained	11.34 kN
Bolts per side plate	2 × M16
Hole diameter dn	18 mm
Wall thickness t	12 mm
End distance e1	90 mm
Pitch s	80 mm
Side distance e2	70 mm
Effective width w	140 mm
Backing-plate diameter / width used for local screening	80 mm

Table 4. Geometry and actions for one U1 side plate and connected column face.

Limit state	Basis	Rd short, kN	Util. short	Rd sustained, kN	Util. sustained
Bearing	Per face	34.56	0.51	13.82	0.82
Net-section tension	Per face	40.32	0.43	16.13	0.70
Shear-out / longitudinal splitting	Per face	30.43	0.57	12.17	0.93
Cleavage, Eq. (8)	Per face	30.40	0.58	12.16	0.93
Cleavage at leading bolt, Eq. (9)	Per bolt	15.05	0.58	6.02	0.94
Block shear	Per face	99.58	0.18	39.83	0.28
Bolt shear, class 8.8	Per face	120.58	0.15	120.58	0.09

Table 5. Complete strength screening of U1. Utilization is demand divided by design resistance.

The sustained-load check governs. The highest utilization is 0.94 for the cleavage expression applied to the leading bolt; shear-out and the alternative cleavage expression follow closely at 0.93. This outcome is materially different from the bearing-only result: edge distance, pitch, and the time-effect factor control the detail. A reduction of e1 or s, omission of the internal plate, or allowing threads to enter the bearing zone would invalidate the stated capacity.

Interlaminar separation is not represented by a complete fracture-mechanics model because the benchmark does not specify the laminate lay-up or a measured interlaminar toughness. It is nevertheless screened quantitatively. The average ring shear around an 80 mm backing plate is $\tau_{ring} = V_{bolt}/(\pi D_{pt}) = 2.90$ MPa under the short-duration action and 1.88 MPa under sustained action. Against $0.5F_{sh} = 12.5$ MPa and $\lambda 0.5F_{sh} = 5.0$ MPa, the corresponding ratios are 0.23 and 0.38. These low average values support

ISSN: 2181-3337 | SCIENTISTS.UZ

the plate size, but they do not capture peak stresses or washer pull-through. Qualification to ASTM D7332 and a full-scale U1 test therefore remain mandatory (ASTM International, 2023b).

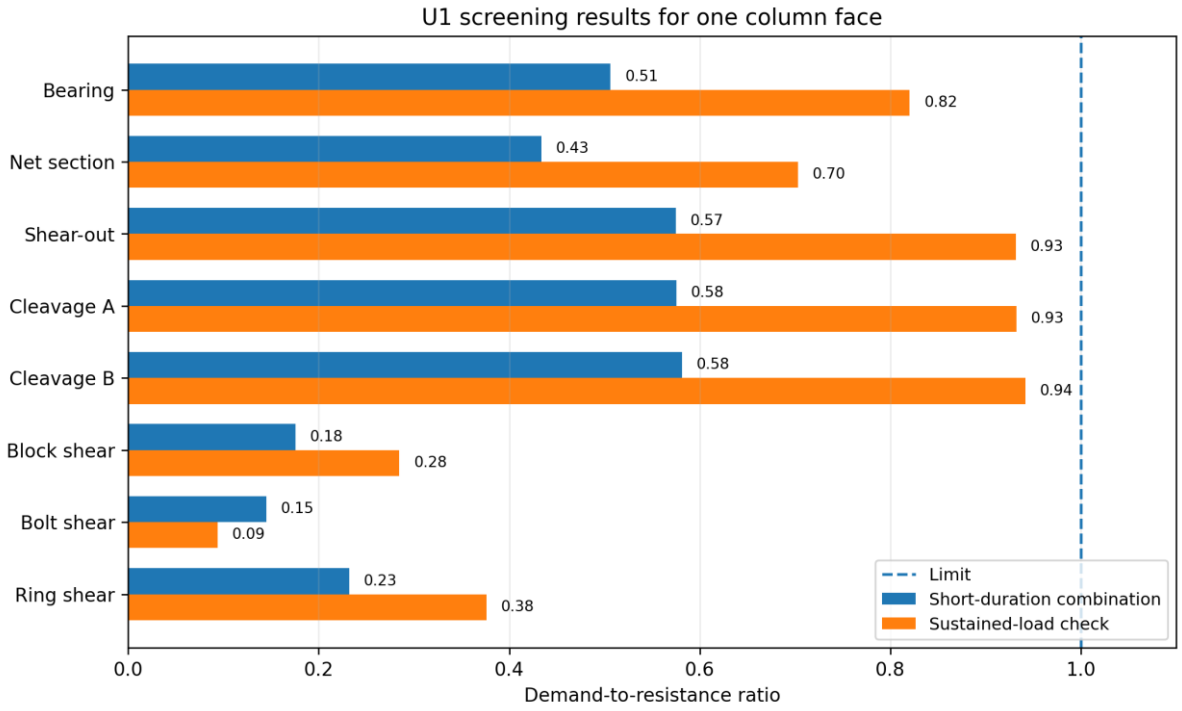


Figure 3. Demand-to-resistance ratios for the revised U1 detail.

4.2. U2 lower supports

The wall module is carried by four adjustable shoes. Side anchors do not carry permanent vertical force, which avoids frictional binding in their slots. The 7.46 kN design reaction is the input for the shoe plate, anchorage, and local wall cassette. With a nominal 120 × 80 mm contact area, the mean pressure is 7.46/0.0096 = 0.78 MPa. The bearing cassette must engage both printed shells or a locally densified core zone; transferring this pressure through one 30 mm shell is not permitted.

Drainage is part of the structural detail. The shoe is separated from the printed material by a waterproof, non-creeping pad; the lower edge drains outward; and the adjustment screw remains accessible. The façade sealant is not used as a bearing material. These measures prevent water accumulation at a point where repeated wetting, freezing, and local pressure would otherwise act together.

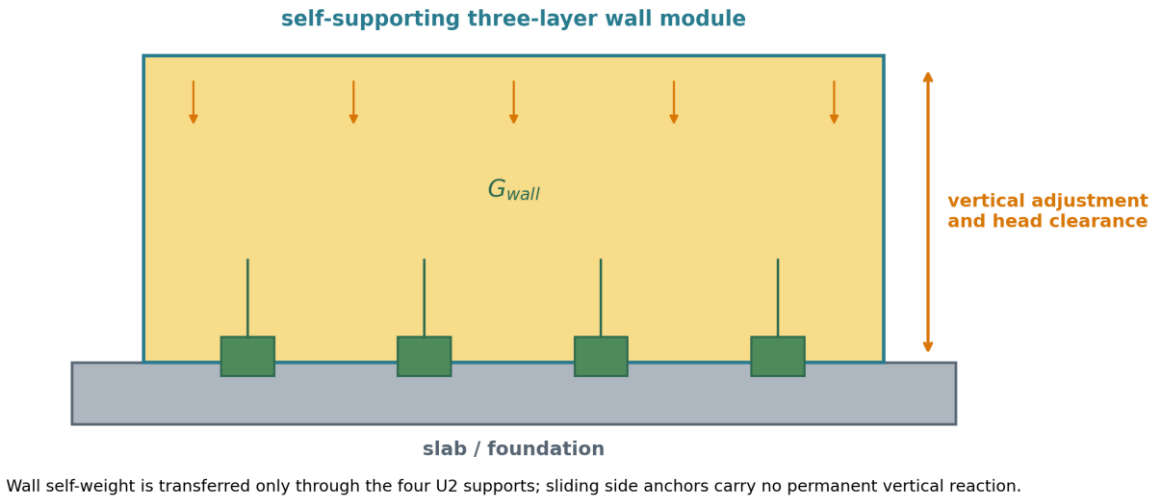


Figure 4. Separate transfer of wall self-weight through four U2 supports.

ISSN: 2181-3337 | SCIENTISTS.UZ

4.3. U3-U4 sliding restraints

The total out-of-plane force on one wall module is 12.96 kN. With six side anchors and the 1.50 distribution factor, one anchor is designed for 3.24 kN in either pressure direction. The embedded cassette must distribute this force over several printed beads and must engage the core mechanically; an adhesive film may improve contact but is not treated as the sole pull-out mechanism.

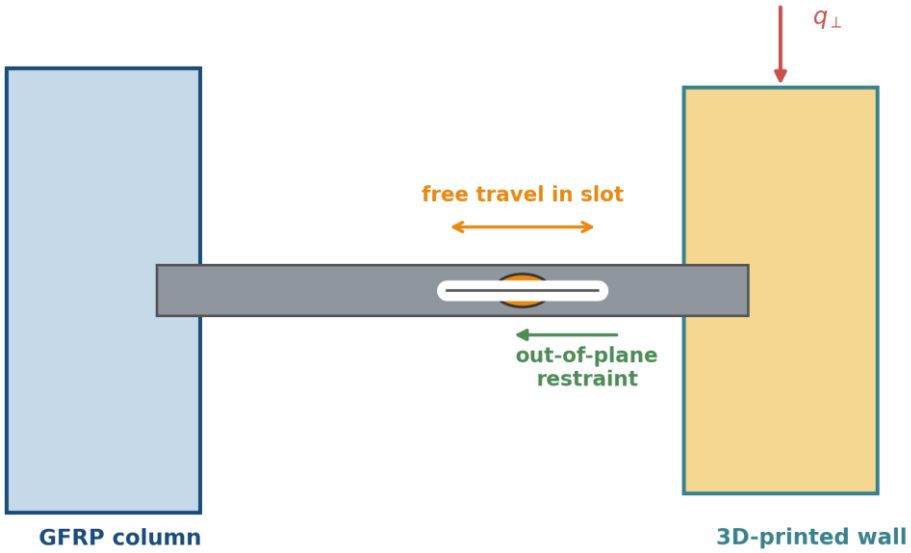


Figure 5. Sliding restraint: out-of-plane stiffness is retained while in-plane movement occurs in the slot.

Travel component	Value, mm	Basis
Interstory drift	30.00	1.0% × 3000 mm
Thermal movement	1.08	10×10^{-6}/K × 30 K × 3600 mm
Wall shortening allowance	1.44	0.0004 × 3600 mm
Erection tolerance	5.00	Printing, cassette, drilling, and frame alignment
Elastic-compliance credit	0.00	No unverified deduction
Required one-sided travel g	37.52	Sum of the above
Calculated slot length	89.04	14 + 2g
Adopted slot length	95	Rounded manufacturing reserve

Table 6. Derivation of the sliding-anchor free travel and slot length.

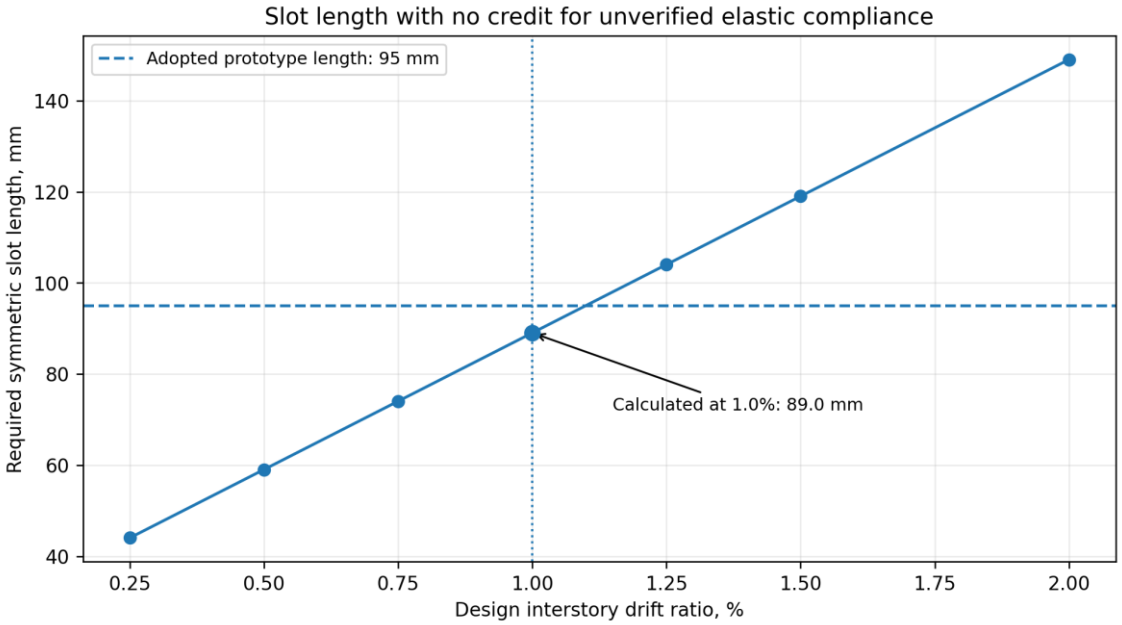


Figure 6. Required slot length as a function of the design drift ratio.

A drawing dimension alone does not guarantee movement capacity. After installation, the bolt position is measured from both slot ends and the actual positive and negative travel is recorded at the installation temperature. Mortar, sealant, a distorted washer, or a rotated cassette can consume the reserve even when the nominal slot is 95 mm. The acceptance quantity is therefore residual travel, not slot length by itself.

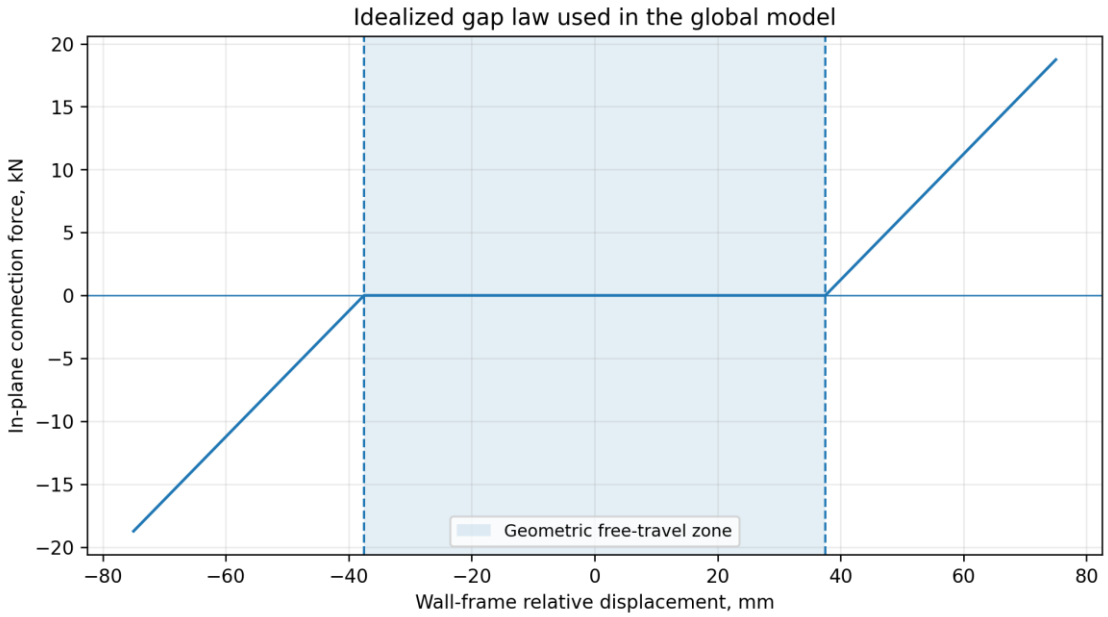


Figure 7. Piecewise force-displacement law used for the in-plane connection response.

4.4. Limit on unintended wall participation

The 10% criterion is not treated as a code limit. It is derived from a modeling tolerance. If the bare frame has stiffness Kf and the wall adds Kw before the gap is exhausted, the period ratio is $T_{coupled}/T_{frame} = 1/\sqrt{(1 + K_w/K_f)}$. Limiting the reduction of the fundamental period to 5% gives $K_w/K_f \leq 1/0.95^2 - 1 = 0.108$. A rounded limit $\beta = 0.10$ is used in the benchmark.

ISSN: 2181-3337 | SCIENTISTS.UZ

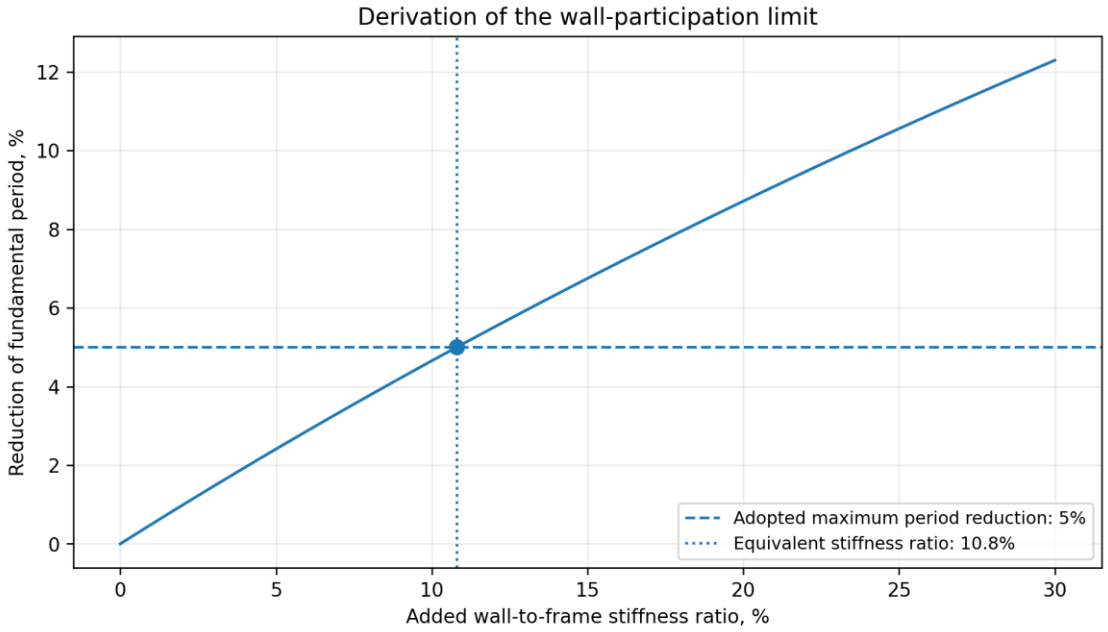


Figure 8. Relationship between unintended added stiffness and the reduction of the frame period.

For Vstory = 28.0 kN and Δd = 30 mm, the equivalent initial stiffness permitted before the design state is:

$$Kallow = \beta Vstory/\Delta d = 0.10(28.0)/30 = 0.093\ kN/mm \quad (13)$$

This small value explains why a nominally flexible bracket is not enough. A bracket with K = 0.20 kN/mm would transfer 6.0 kN at 30 mm, or 21.4% of the story shear. The geometric gap makes the pre-contact stiffness essentially zero and is therefore the controlling design feature.

4.5. Connection-option screening without subjective weights

Comparative test data, life-cycle cost data, and an agreed expert-elicitation procedure are not available; consequently, a weighted numerical score would suggest a precision that the evidence does not support. Connection concepts are therefore screened by mandatory pass/fail constraints. An option is retained only if it provides the required geometric travel, carries out-of-plane force independently of wall weight, permits inspection, and does not rely on an unverified adhesive path.

Concept	Geometric free travel ≥ g	Separate self-weight path	Inspection / repair	Screening decision
Rigid steel bracket	No	Possible	Good	Excluded: engages wall from zero displacement
Slotted GFRP bracket	Yes	Yes	Conditional	Candidate; slot wear and creep require testing
Adhesively bonded tie	No controlled gap	No	Poor	Excluded as the primary movement detail
Hybrid bonded-bolted tie	Limited / uncertain	Possible	Moderate	Conditional; not selected for benchmark
Sliding cassette with replaceable bracket	Yes	Yes	Good	Retained for prototype evaluation

Table 7. Deterministic screening of connection concepts. No claim of universal superiority is made.

ISSN: 2181-3337 | SCIENTISTS.UZ

5. Detailing, construction control, and serviceability

5.1. Installation sequence

Installation begins with a geodetic survey of the frame and the U2 support elevations. The wall is placed on the four shoes, adjusted to line and level, and temporarily restrained. U3-U4 bolts are then placed at their temperature-corrected initial positions in the slots. Only after positive and negative travel has been measured are the movement joints sealed. This order prevents finishes from hiding a blocked slot.

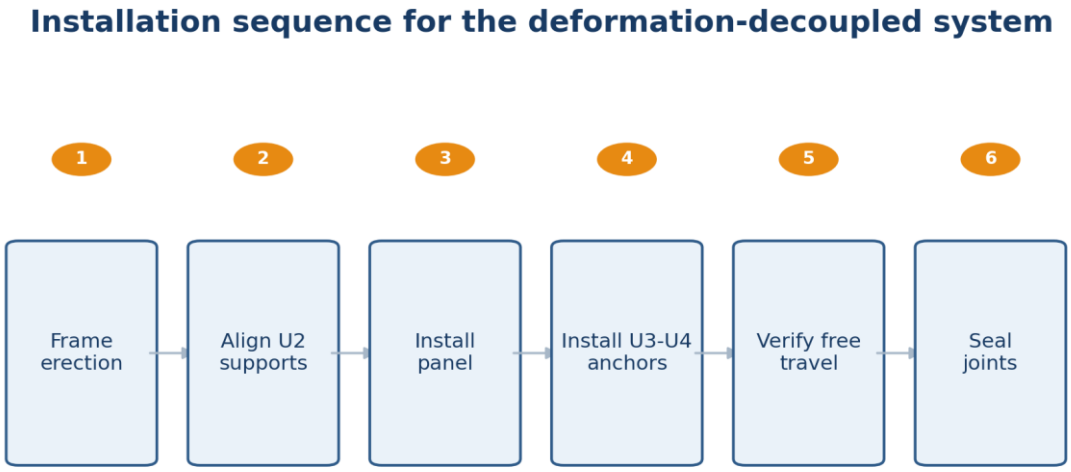


Figure 9. Recommended installation sequence for the deformation-decoupled interface.

Stage	Controlled quantity	Acceptance record
GFRP profile and U1 drilling	Batch, orientation, hole diameter, ovality, edge distances, visible delamination	Profile ID, measured geometry, photographs
U1 backing plates and sleeves	Plate dimensions; full contact; sleeve length equal to clear internal dimension	Actual plate and sleeve dimensions
U1 bolt installation	Unthreaded shank in bearing zone; calibrated tightening; no wall indentation	Bolt batch, method, torque / tension value
U2 supports	Elevation, engaged contact area, drainage, pad condition	Four support levels and final wall verticality
U3-U4 slots	Length, width, orientation, bolt position, washer clearance	Actual + and - residual travel at recorded temperature
U5 joints	Joint width, backing rod, primer, two-sided adhesion, drainage	Joint geometry and product batch
Final acceptance	Manual proof of travel, out-of-plane restraint, air/water test where required	Panel passport and acceptance sheet

Table 8. Minimum production-control plan for the benchmark connection system.

ISSN: 2181-3337 | SCIENTISTS.UZ

5.2. Thermal, moisture, and fire limitations

Metal components that cross the insulating core create local thermal bridges. The present paper does not assign a numerical U-value increment because the final cassette geometry and contact resistances are not known. A project detail must be checked with a two- or three-dimensional model in accordance with ISO 10211; the minimum internal surface temperature and condensation risk are assessed together with the point or linear transmittance (International Organization for Standardization, 2012, 2017a, 2017b). Massive through-plates should be avoided where a compact component or a GFRP thermal break can transfer the same force.

Moisture control is equally important. Exposed fibers at drilled holes are sealed; the lower support drains; dissimilar metals are isolated; and inspection covers do not create water traps. Low-friction pads in U3-U4 are selected for low creep and compatibility with the expected temperature range. None of these measures is credited as strength without product data.

No fire-resistance rating is claimed. GFRP stiffness and strength can decline at temperatures well below steel melting temperature (Correia et al., 2015). Any rated wall-frame detail requires a continuous protection system and either a validated thermomechanical model or a representative fire test under ISO 834-1 or the applicable national method (International Organization for Standardization, 1999). Fire stopping at a movement joint must preserve the specified travel.

6. Discussion

6.1. Consequences of the complete U1 check

A bearing-only calculation hides two important effects. First, a hollow profile with a washer on only one side of each wall is not equivalent to a laterally restrained coupon. Applying the tube-wall reduction changes the four-bolt detail from apparently adequate to inadequate. Second, the dead-load time-effect factor moves the governing condition from immediate bearing to the edge-sensitive shear-out and cleavage modes. The revised detail is therefore controlled by geometry and load duration rather than by bolt diameter alone.

This result also clarifies the role of the steel seat. The seat transfers the beam reaction through a replaceable component, while the internal plates and sleeves protect the primary composite profile from local crushing. A designer who simply increases bolt torque or adds a larger exterior washer does not create the same load path. The inside face of the tube wall must be engaged.

6.2. Significance of geometric decoupling

The required slot is long because interstory drift dominates the movement budget. Thermal movement and wall shortening contribute only 2.52 mm, yet they cannot be omitted because the installation tolerance acts in the same direction. Assigning no elastic-compliance credit increases the calculated requirement and eliminates dependence on an unmeasured bracket property. The detail is intentionally conservative: compliance may reduce contact force after the gap closes, but it is not used to justify a shorter gap.

The period-based derivation of β provides a rational meaning for the 10% limit. A different project can select another permitted period change and obtain its own β. The method therefore separates a transparent performance choice from the mechanics of the connection. It also makes clear that a low linear spring stiffness is not interchangeable with a true clearance.

6.3. Scope of the analytical result

The benchmark demonstrates a calculation sequence and identifies a buildable prototype. It does not establish characteristic resistance for a commercial profile, a printed mixture, or an embedded cassette. EN 13706 minima are used to avoid invented material properties, but a manufacturer may have different orthotropy, resin, veil, wall architecture, and coefficient of variation. The internal backing-plate assumption, the local interlaminar screening, slot friction, cassette pull-out, and sealing performance are all test-sensitive.

ISSN: 2181-3337 | SCIENTISTS.UZ

The analysis also uses a regular wall without an opening. Corners, windows, doors, and multiple panels can change the local anchor distribution and the global torsional response. The 1.20 kPa pressure and 0.12 lateral coefficient belong only to the stated benchmark. The method remains applicable when those values change, but the numerical results do not.

7. Limitations and planned verification

No experiment has been completed for this paper. Consequently, there are no measured load-displacement curves, repeated specimens, raw data, coefficients of variation, or statistical confidence intervals. The analytical resistances in Table 5 are code-based screening values. They must not be described as experimentally verified, and they are not sufficient for construction approval.

Before a design application, the following program is required. The list is reported as future work and is not part of the present results:

Level	Minimum series	Loading / measurement	Purpose
GFRP material and holes	At least 5 specimens per direction and condition	Tension, pin bearing, short-beam shear; dry and conditioned	Characteristic strengths, scatter, failure mode
U1 subassembly	At least 3 full-scale joints plus geometry variants	Monotonic and reversed cyclic loading; sustained hold	Capacity, slip, cleavage / splitting, sleeve and backing performance
U3-U4 anchor	At least 5 assemblies	3.24 kN out-of-plane action combined with cyclic travel to ±2% drift	Friction, binding, wear, residual travel, cassette pull-out
Wall fragment	At least 3 fragments with a joint and one opening	Cyclic in-plane drift plus pressure and air/water exposure	Cracking, leakage, unintended engagement
Conditioning	Matched conditioned and unconditioned sets	Moisture, temperature cycling, and sustained load	Durability and long-term deformation

Table 9. Planned verification program; no results from these tests are reported in this article.

Statistical treatment should be defined before testing. For each material configuration, the characteristic value, mean, standard deviation, and coefficient of variation are to be reported. For full-scale joints, the complete force-displacement response, residual deformation, failure sequence, and photographs of concealed damage are required. Acceptance criteria cannot be changed retrospectively after an unfavorable result.

8. Conclusions

1. The frame-to-wall interface can be analyzed more clearly when wall weight, out-of-plane restraint, and in-plane movement are assigned to U2, U3-U4, and the movement joints rather than combined in a universal rigid anchor.
2. The key design values are derived from a fixed benchmark. The 35.0 kN U1 reaction follows from a stated tributary area and LRFD combination; 1.20 kPa follows from the declared wind envelope; 28.0 kN follows from the benchmark story weight and lateral coefficient; and the 10% participation limit follows from a 5% cap on period reduction.

ISSN: 2181-3337 | SCIENTISTS.UZ

3. A conventional four-bolt through-connection in an unsupported hollow GFRP wall is inadequate when the ASCE/SEI 74-23 tube-wall and time-effect reductions are applied. The revised seat detail uses internal backing plates, sleeves, and an unthreaded bolt shank in the bearing zone.
4. For one revised U1 side plate, bearing, net-section tension, shear-out, cleavage, block shear, bolt shear, and a local interlaminar-stress screening were evaluated. The maximum short-duration utilization is 0.58; the maximum sustained-load utilization is 0.94 and occurs at the leading-bolt cleavage check.
5. The 3.6 × 3.0 m wall module has a factored weight of 22.95 kN. Four lower supports are designed for 7.46 kN each, while six side restraints are designed for 3.24 kN each under the stated 1.20 kPa envelope.
6. With no credit for unverified elastic compliance, the required one-sided in-plane travel is 37.52 mm. A 14 mm wide slot requires 89.04 mm analytically; 95 mm is adopted, and actual positive and negative residual travel must be measured after installation.
7. The study reports an analytical result only. Product certification, full-scale U1 testing, combined U3-U4 cycling, wall-fragment testing, and statistical evaluation remain necessary before the system can be used in a construction project.

Declarations

Author contributions. D.B.A.: conceptualization, analytical methodology, calculations, visualization, and preparation of the original manuscript. K.A.A.: scientific supervision, methodological review, interpretation of the structural results, and review and editing of the manuscript.

Funding. This research received no external funding.

Conflicts of interest. The authors declare no conflict of interest.

Data availability. No experimental dataset was generated. All benchmark inputs, equations, intermediate quantities, and analytical results used in the paper are reported in Tables 2-9.

Ethics statement. Not applicable.

REFERENCES

1. American Society of Civil Engineers. (2022). *Minimum design loads and associated criteria for buildings and other structures* (ASCE/SEI 7-22). https://doi.org/10.1061/9780784415788
2. American Society of Civil Engineers. (2023). *Load and resistance factor design (LRFD) for pultruded fiber reinforced polymer (FRP) structures* (ASCE/SEI 74-23). https://doi.org/10.1061/9780784415771
3. ASTM International. (2023a). *Standard test method for bearing response of polymer matrix composite laminates* (ASTM D5961/D5961M-23).
4. ASTM International. (2023b). *Standard test method for measuring the fastener pull-through resistance of a fiber-reinforced polymer matrix composite* (ASTM D7332/D7332M-23).
5. Bank, L. C. (2006). *Composites for construction: Structural design with FRP materials*. John Wiley & Sons.
6. Bos, F. P., Menna, C., Pradena, M., et al. (2022). The realities of additively manufactured concrete structures in practice. *Cement and Concrete Research, 156*, 106746. https://doi.org/10.1016/j.cemconres.2022.106746
7. Correia, J. R., Bai, Y., & Keller, T. (2015). A review of the fire behaviour of pultruded GFRP structural profiles for civil engineering applications. *Composite Structures, 127*, 267–287. https://doi.org/10.1016/j.compstruct.2015.03.006
8. Erdem, M. M., Emsen, E., & Bikçe, M. (2021). Experimental and numerical investigation of new flexible connection elements between infill walls and reinforced-concrete frames. *Construction and Building Materials, 296*, 123605. https://doi.org/10.1016/j.conbuildmat.2021.123605

ISSN: 2181-3337 | SCIENTISTS.UZ

9. Eskenati, A. R., Mahboob, A., Bernat-Maso, E., & Gil, L. (2022). Experimental and numerical study of adhesively and bolted connections of pultruded GFRP I-shape profiles. *Polymers, 14*, 894. https://doi.org/10.3390/polym14050894
10. European Committee for Standardization. (2002). *Reinforced plastics composites—Specifications for pultruded profiles* (EN 13706-1/-2/-3).
11. European Committee for Standardization. (2005). *Eurocode 3: Design of steel structures—Part 1-8: Design of joints* (EN 1993-1-8:2005).
12. European Committee for Standardization. (2022). *Design of fibre-polymer composite structures* (CEN/TS 19101:2022).
13. Federal Emergency Management Agency. (2012). *Reducing the risks of nonstructural earthquake damage: A practical guide* (FEMA E-74).
14. Girão Coelho, A. M., & Mottram, J. T. (2015). A review of the behaviour and analysis of bolted connections and joints in pultruded fibre reinforced polymers. *Materials & Design, 74*, 86–107. https://doi.org/10.1016/j.matdes.2015.02.011
15. International Organization for Standardization. (1999). *Fire-resistance tests—Elements of building construction—Part 1: General requirements* (ISO 834-1:1999).
16. International Organization for Standardization. (2012). *Hygrothermal performance of building components and building elements—Internal surface temperature to avoid critical surface humidity and interstitial condensation* (ISO 13788:2012).
17. International Organization for Standardization. (2017a). *Building components and building elements—Thermal resistance and thermal transmittance—Calculation methods* (ISO 6946:2017).
18. International Organization for Standardization. (2017b). *Thermal bridges in building construction—Heat flows and surface temperatures—Detailed calculations* (ISO 10211:2017).
19. International Organization for Standardization & ASTM International. (2023). *Additive manufacturing for construction—Qualification principles—Structural and infrastructure elements* (ISO/ASTM 52939:2023).
20. Martins, D., Gonilha, J., Correia, J. R., & Silvestre, N. (2021a). Exterior beam-to-column bolted connections between GFRP I-shaped pultruded profiles using stainless steel cleats. Part 1: Experimental study. *Thin-Walled Structures, 163*, 107719. https://doi.org/10.1016/j.tws.2021.107719
21. Martins, D., Gonilha, J., Correia, J. R., & Silvestre, N. (2021b). Exterior beam-to-column bolted connections between GFRP I-shaped pultruded profiles using stainless steel cleats. Part 2: Prediction of initial stiffness and strength. *Thin-Walled Structures, 164*, 107762. https://doi.org/10.1016/j.tws.2021.107762
22. Martins, D., Gonilha, J., Correia, J. R., Silvestre, N., Guerreiro, L., & Branco, F. (2023). Monotonic and cyclic sway behaviour of two-dimensional frames made of pultruded GFRP I-section profiles. *Structures, 55*, 2461–2477. https://doi.org/10.1016/j.istruc.2023.07.035
23. Matharu, N. S., & Mottram, J. T. (2017). Plain and threaded bearing strengths for the design of bolted connections with pultruded FRP material. *Engineering Structures, 152*, 878–887. https://doi.org/10.1016/j.engstruct.2017.10.003
24. Pirchio, D., Althouse, J. A., Madlem, T. A., Denavit, M. D., & Walsh, K. Q. (2024). Assessment of resistance factors for LRFD of steel-bolted connections in pultruded FRP frames. *Journal of Composites for Construction*. https://doi.org/10.1061/JCCOF2.CCENG-4104
25. Qureshi, J. (2022). A review of fibre reinforced polymer structures. *Fibers, 10*, 27. https://doi.org/10.3390/fib10030027
26. Qureshi, J., Nadir, Y., & John, S. K. (2020). Bolted and bonded FRP beam-column joints with semi-rigid end conditions. *Composite Structures, 247*, 112500. https://doi.org/10.1016/j.compstruct.2020.112500

ISSN: 2181-3337 | SCIENTISTS.UZ